Korean J. Chem. Eng., 32(7), 1427-1433 (2015)
DOI: 10.1007/s11814-014-0355-1

pISSN: 0256-1115
eISSN: 1975-7220

Synthesis and properties of amino acid functionalized water-soluble perylene diimides

Yongshan Ma†, Xuemei Li, Xiaofeng Wei, Tianyi Jiang, Junsen Wu, and Huixue Ren

School of Municipal and Environmental Engineering, Shandong Jianzhu University, Jinan 250101, P. R. China
(*Received 30 May 2014 • accepted 1 December 2014*)

Abstract−We prepared amino acid functionalized water-soluble perylene diimides: N,N′-bi(L-glutamic acid)-perylene-3,4;9,10-dicarboxylic diimide (**1**), N,N′-bi(L-phenylalanine acid)-perylene-3,4;9,10-dicarboxylic diimide (**2**), N,N′-bi(L-glutamic amine)-perylene-3,4;9,10-dicarboxylic diimide (**3**) and N,N′-bi(L-phenylalanine amine)-perylene-3,4;9,10-dicarboxylic diimide (**4**). The structures of **3** and **4** were confirmed by ^{1}H NMR, FT-IR and MS. The maximal absorption bands of compound **1** and **2** in concentrated sulfuric acid were red-shifted for about 48 and 74 nm, respectively, compared with that of Perylene-3,4,9,10-tetracarboxylic acid dianhydride (PTCDA). Nearly no fluorescence was observed for compounds **1** and **2** in water, while compounds **3** and **4** were significantly water-soluble and had very high fluorescent quantum. The mechanism of the optical properties change was discussed, and the π-π stacking caused by H^+ led to the changes of fluorescence spectrum and absorption spectrum. The calculated molecular orbital energies and the frontier molecular orbital maps of compounds **1**-**2** based on density function theory (DFT) calculations were reported. Owing to the high water-soluble, the perylene derivatives **3** and **4** were successfully applied as high-performance fluorochromes for living hela cells imaging.

Keywords: Water-soluble Perylene Diimides, Synthesis, Absorption Spectrum, Fluorescence Spectrum, DFT Calculations, Living Cell Staining

INTRODUCTION

Perylene diimides (PDIs) are highly versatile dyes and pigments with various applications such as molecular switches, organic light-emitting diodes, photoreactive thin films, light-harvesting arrays, dye lasers and solar cells [1-6]. Recently, perylene dyes have been proven to be cell-permeable and used for live-cell imaging [7,8]. However, the solubility of PDIs is generally poor because of their tendency to aggregate even at very low concentrations in aqueous solutions [9]. It is highly desirable to obtain water-soluble PDIs for their potential biological applications. The modification on molecular structure of PDIs is usually achieved by introducing side groups to the bay position or at the imide nitrogen atom. Substitution at the bay position can increase the solubility of PDIs in organic solvents, but will change their photophysical properties [10]. Simple substitution at the imide groups can affect the packing behavior of PDIs in the solid state, improving the solubility of PDIs in solvents, without changing their photophysical properties significantly [11]. Recently, Gao et al. reported dendritic perylene bisimide probes with triblock structures: branched oligo(glutamic acid)s, perylene bisimides fluorescence cores and polyethylene glycol chains at the imide groups. These probes showed good water solubility and strong fluorescence [12]. Maria, et al. reported a set of highly water-soluble bolaamphiphilic PDIs which were simply and easily synthesized [13]. Furthermore, low cytotoxicity PDIs with high fluorescence in water are highly desired [14].

In this paper, we synthesized two amino acid functionalized water-soluble perylene diimides: N,N′-bi(L-glutamic acid)-perylene-3,4;9,10-dicarboxylic diimide(compound **1**) and N,N′-bi(L-phenylalanine acid)-perylene-3,4;9,10-dicarboxylic diimide (compound **2**). Then, compound **1** and **2** can further react with $NH_3 \cdot H_2O$ to create new compound: N,N′-bi(L-glutamic amine)-perylene-3,4;9,10-dicarboxylic diimide(compound **3**) and N,N′-bi(L-phenylalanine amine)-perylene-3,4;9,10-dicarboxylic diimide (compound **4**) (Fig. 1). Owing to the high negative electrostatic potential of the perylene plane, the resulting new compounds **3** and **4** showed significant solubility in water and yielded very high fluorescent quantum. These two compounds were successfully applied as high-performance fluorochrome for living cervical cancer cells imaging.

EXPERIMENTAL

1. Materials and General Methods

PTCDA, L-glutamic amine, L-phenylalanine amine, dimethyl sulfoxide, ethanol (DMSO), hydrochloric acid, and sodium hydroxide were of reagent grade and purchased from commercial source.

The ^{1}H NMR spectra (chemical shifts are reported in ppm) were recorded on a Bruker INOVA 400-MHz spectrometer. FT-IR spectra were recorded on a Bruker TENSOR-27 spectrometer. Mass spectra were taken on a Thermo Finnigan ESI instrument (data were presented in m/z (%) values). UV-Vis absorption spectra were measured on a Varian CARY-50 spectrophotometer. Fluorescence spectra were performed on a Hitachi FL-4500 PC spectrofluorophotometer. The cells were observed and photographed on an Olympus BH-2 fluorescence microscope.

2. Computation Details

Becke's three parameter gradient-corrected hybrid density function B3LYP method [15,16] and the standard 6-31G(d) basis set

†To whom correspondence should be addressed.
E-mail: mlosh@sdjzu.edu.cn

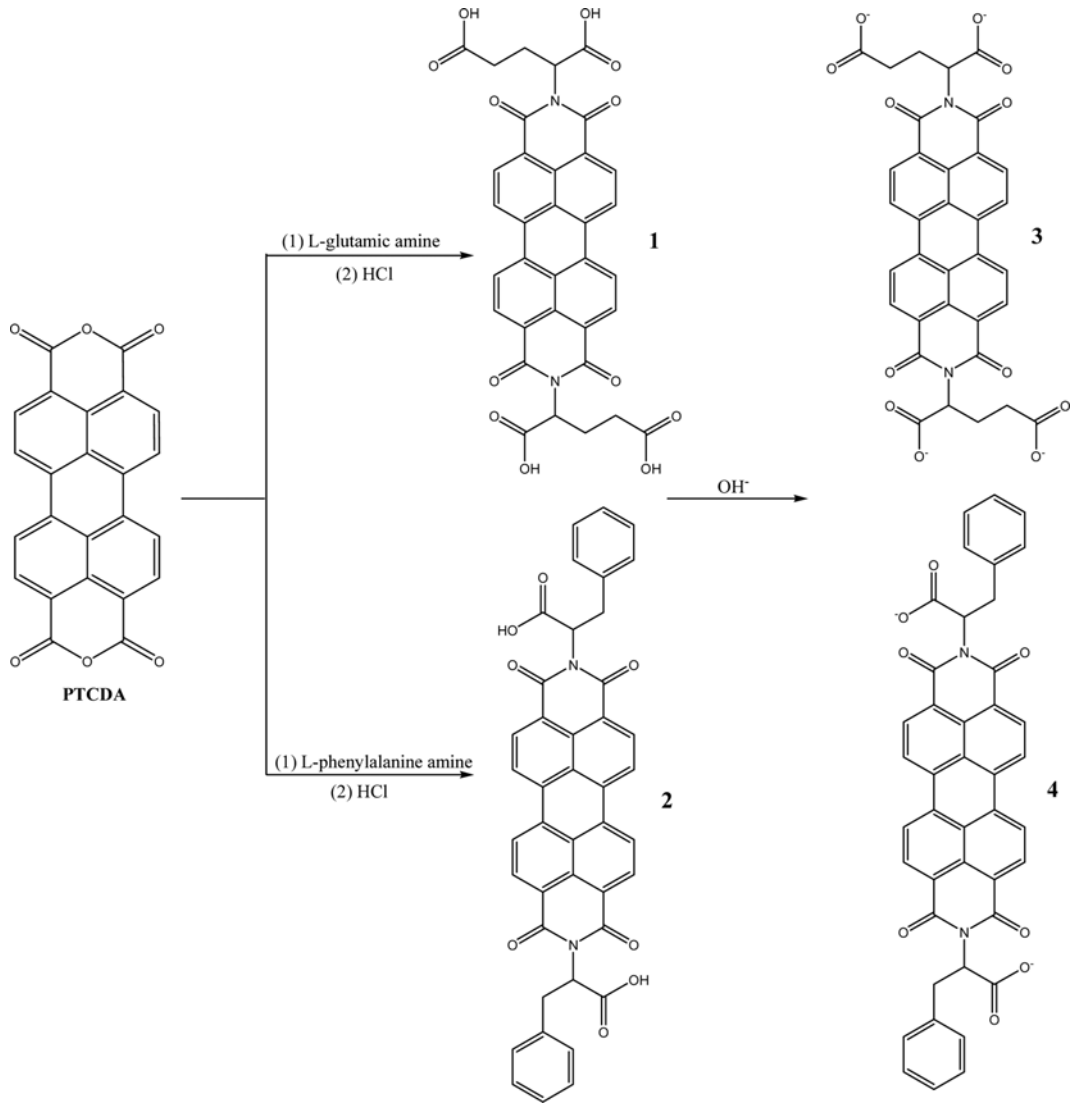

Fig. 1. Synthesis of compound 1-4.

[17] were used for both structure optimization and the property calculations. All the calculations were performed using the Gaussian 03 program installed on a Windows PC.

3. Synthesis and Analytical Methods

3-1. Compound **1** and **3**

The preparation of compound **1** followed the procedure presented in previous literature [18,19]: A mixture of L-glutamic amine (4.0 g, 24 mM) and PTCDA (0.6 g, 1.6 mM) was dissolved in 60 ml of DMSO and heated at reflux for 4 h. After being cooled to room temperature and centrifuged, the precipitate was washed with 45 ml of ethanol (3×15 ml) and then dissolved in 60 ml of water. When the solution pH was adjusted to 1 with diluted hydrochloric acid, the precipitate was separated out. The crude product of compound **1** was further purified by dissolving in 100.0 mL DMF then added diluted hydrochloric acid to adjust pH~1; dissolving in 100.0 mL KOH solution (9.0 mmol, 505 mg) and then precipitated by dropwise adding of diluted hydrochloric acid to pH~1. Then, the compound **1** was obtained by being filtered and washed with 90 ml of diluted hydrochloric acid (3×30 ml) and 90 mL of ethanol (3×30 ml). The intermediate product was neutralized with 15 ml of 15% $NH_3 \cdot H_2O$ and stirred at room temperature for 10 min. The precipitate was filtered off as solvent being evaporated. Then compound **3** was obtained as a brown powder (0.7 g, 72% yield) with being dried at 100 °C under vacuum. Characterization data: **3**: ^{1}H-NMR (D_2O, TMS, ppm): δ_H 8.38 (d, J=14.8 Hz, 4H), 8.16 (d, J=15.0 Hz, 4H), 6.32 (t, J=14.5 Hz, 2H), 2.69-2.56 (m, 4H), 2.45-2.20 (m, 4H) (Fig. 2). FT-IR (cm^{-1}): v 3433, 3164, 3052, 2847, 1689, 1592, 1361, 1345, 1273, 1182, 1114, 1021, 951, 853, 809, 793, 737, 659, 461, 432. MS (EI): (m/z): 646.2 $[M]^+_o$

3-2. Compounds **2** and **4**

A mixture of L-phenylalanine (3.30 g, 20 mmol) and potassium hydroxide (1.12 g, 20 mmol) in 20 ml of water was stirred for 2 h at room temperature, and then excess water was removed on a rotary evaporator to afford L-phenylalanine amine (4.06 g). Then compounds **2** and **4** were synthesized as the procedure of synthesis of **1** and **3**. 0.8 g PTCDA and 4.06 g L-phenylalanine amine reacted for 6 h in DMSO to yield **2.** Compound **2** reacted with 15% $NH_3 \cdot H_2O$ for 10 min to give a reddish brown powder **4** (0.75 g, 40%).

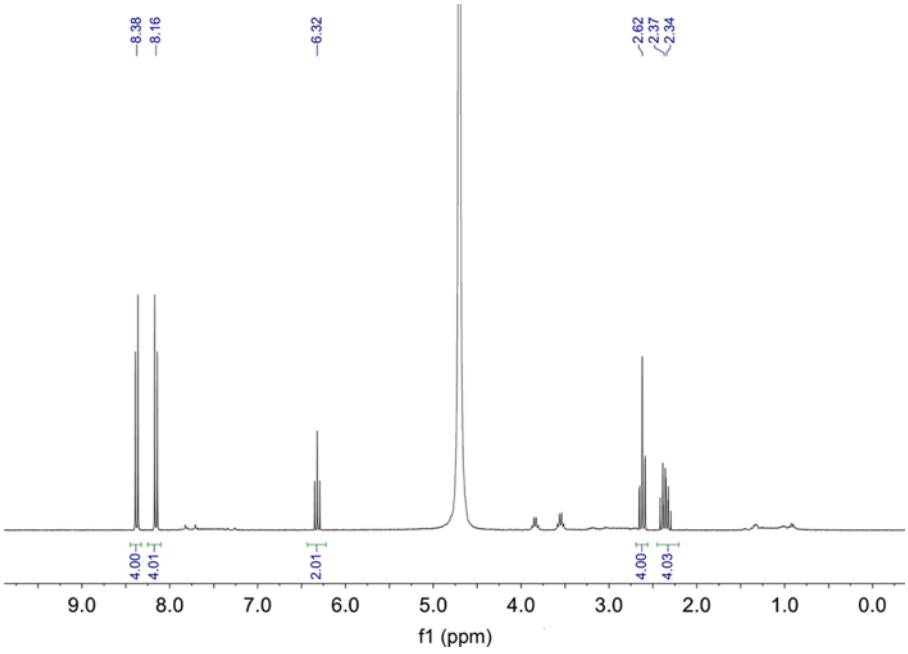

Fig. 2. ^{1}H-NMR spectrum of compound 3.

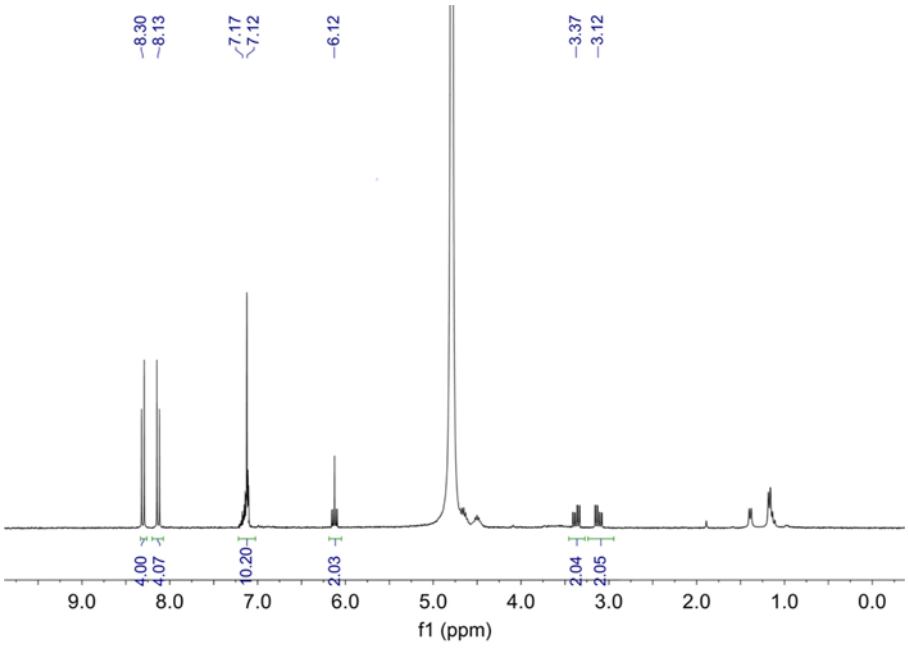

Fig. 3. ^{1}H-NMR spectrum of compound 4.

Characterization data: **4**: ^{1}H-NMR (D_2O, TMS, ppm): δ_H 8.31 (d, J=15.0 Hz, 4H), 8.13 (d, J=14.8 Hz, 4H), 7.22-7.02 (m, 10H), 6.19-6.05 (m, 2H), 3.46-3.27 (m, 2H), 3.24-2.94 (m, 2H) (Fig. 3). FT-IR (cm^{-1}): v 3443, 3163, 3052, 2846, 1690, 1592, 1399, 1361, 1273, 1182, 1114, 1021, 951, 853, 809, 793, 737, 659, 461, 432. MS(EI): (m/z): 624.2 $[M]^+_o$

4. Cell Culture for HeLa Cell

HeLa cells were seeded and grown in Dulbecco's modified Eagle's medium supplemented with 10% foetal bovine serum at 37 °C, and 10^4 cells were added in each well in a 24-well culture plate. After 48 h of growth, the hela cells were stained by compounds 3 or 4 (10^{-5} M) for 1.0 h and then washed by phosphate-buffered saline (PBS) twice to remove remaining probes. Cells were viewed under fluorescence microscope at an excitation with a UV-filter source of 330-380 nm.

RESULTS AND DISCUSSION

1. Synthesis

The chemical structure of compounds **1**-**4** and their synthetic

routes are shown in Fig. 1. Compounds **1** and **2** were synthesized following a modified literature method [18,19]. Perylene-3,4,9,10-tetracarboxylic acid dianhydride (PTCDA) with L-glutamic amine or L-phenylalanine amine was carried out under reflux using dimethylsulfoxide as solvent. To obtain compounds **1** or **2**, extra excess of amine and shorter reaction time compared with that of the literature method were necessary. Compounds **1** and **2** further react with $NH_3 \cdot H_2O$ at room temperature for 10 min to give **3** and **4** with yields of 72% and 40%, respectively. Both compounds **3** and **4** show good solubility in water and N,N-dimethylformamide solvents, but small solubility in alcoholic and chloroform solvents. The structures of compounds **3** and **4** were fully characterized by different spectroscopic methods, including ^{1}H NMR, FT-IR and MALDI-TOF mass spectrometry. It is reasonable to expect the formation of compounds **1** and **2** due to the newly formed compounds **3** and **4**. However, the ^{1}H NMR spectra did not show any evidence to support the presence of compounds **1** and **2** for their poor solubility in D_2O. This may be ascribed to the π-π stacking produced by H^+ at carboxyl group for its electron accepting nature.

2. Optical Properties

Fig. 4 compares the electronic absorption spectra of compounds **1** and **2** with model compound PTCDA in concentrated sulfuric acid. All these compounds show good solubility and intense absorption in the UV-Vis region. The maximal absorption bands of PTCDA were 500 and 546 nm. Compounds **1** and **2** exhibit absorption band peaks at 594 nm (ε=1.12×10^5 L cm^{-1}mol^{-1}) and 620 nm (ε=1.81×10^5 L cm^{-1}mol^{-1}), respectively, with characteristic vibronic structure that were attributed to π-π* transitions localized on the perylene core. The maximal absorption bands of compounds **1** and **2** are red-shifted for about 48 nm and 74 nm, respectively, compared with that of PTCDA. These findings suggest there is photoinduced intramolecular charge transfer in compounds **1** and **2**. Electron deficient nature of perylene core initiates the movement of electron density from the electron donors (nitrogen atom) located in imide positions to the perylene core, then the polarizability of the whole molecule changes in the excited state, leading to significant red-shift on their absorption spectra. The red-shift of the maximal

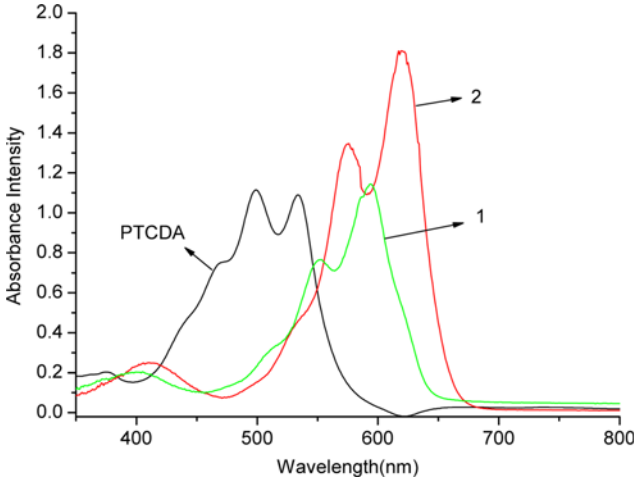

Fig. 4. Absorption spectra of compounds 1 and 2 compared with that of PTCDA in concentrated sulfuric acid (10^{-5} M).

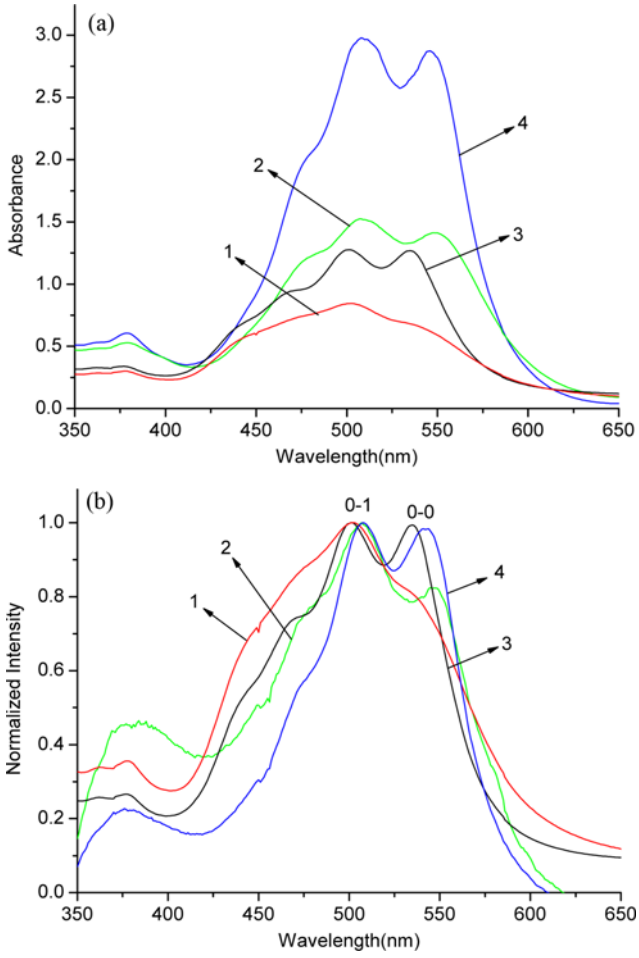

Fig. 5. Absorption spectra (a) and normalized absorption spectra (b) of compounds 1-4 in aqueous solution (5×10^{-5} M).

absorption band of compound **2** is 26 nm larger than that of compound **1**. As an L-phenylalanine amine substituted derivative, **2** was a comparative electron donor of **1**.

The UV-Vis absorption spectra of **1**-**4** in aqueous solution are shown in Fig. 5(a). In the absence of any substituent in the bay positions, their PDI cores are nearly planar. However, the optical properties of them in solution and in aggregation state are significantly different. Generally, in solution, the PDIs are characterized by two absorption bands which are assigned to the 0-0 and 0-1 electronic transitions. Passing from solution to aggregate state, the 0-1 transition increased and the relative intensity of these absorption bands reverses. There is a loss of the fine vibronic structure and the spectra become more broadened. This is an indication that the PDIs molecular scaffolds allow π-π intermolecular interactions, inducing molecular aggregation [20,21]. This is a usual behavior for perylene diimide systems. It is well known that the π-π intramolecular interactions have a strong influence on PDI optical properties.

Compounds **1** and **2** in aqueous solution exhibit absorption in the visible range with wavelength maxima at 533 nm (ε=1.4×10^4 L cm^{-1}mol^{-1}) and 544 nm (ε=2.8×10^4 L cm^{-1}mol^{-1}), which are blue-shifted for about 61 and 76 nm, respectively, compared with that in concentrated sulfuric acid. It can be ascribed to the formation

of H-type aggregates in aqueous solution [22,23], which was caused by the π-π electronic coupling between PDI chromophores and/or hydrophobic interaction in water. Absorption spectra in Fig. 5(a) give a convincing evidence. The absorption bands at 533 nm and 502 nm of compound **1** are assigned to the 0-0 and 0-1 electronic transitions of the PDI chromophore. They decreased remarkably in aqueous solution than in concentrated sulfuric acid. Moreover, the relative intensity of 0-0 and 0-1 bands reverses as in aqueous solution. Such a change indicates strong molecular aggregation in aqueous solution induced by π-π stacking. Similar appearance was also observed in the spectra of compound **2**.

There is a loss of the fine vibronic structure of compound **1** and the spectra become more broadened, while the absorption spectrum of the compound **2** figure out the neat three vibronic maxima of characteristic PDI monomer absorption, and there is no observation of a broadened spectrum. Zhu et al. reported an aspartic acid-functionalized water-soluble perylene bisimide, N,N′-di(2-succinic acid)-perylene-3,4,9,10-tetracarboxylic bisimide (PASP), which was similar to compound **1** [19]. PASP contains four acid substitutes, so full deprotonation of PASP needs higher pH (>7.64). Aggregation reaction (from monomer) was quite slow compared with deprotonation reaction. There were still some aggregations in pH 7.20-8.52. Compound **2** contains only two acid substitutes, so its full deprotonation needs lower pH. This may explain why the compound **2** figure out the neat three vibronic maxima, and there is no observation of a broadened spectrum, indicating the negative charges in the phenylalanine moiety do not favor aggregation form of compound 2.

Since we were interested in showing the peak shapes, the UV-Vis absorption spectra of **1**-**4** were normalized to unity (Fig. 5(b)). In aqueous solution, compounds **3** and **4** exhibit absorptions in the visible range with peak maxima at 533, 502 nm and 544, 508 nm, respectively. From **1** to **3**, the 0-1 transition absorption of **3** decreased relatively, indicating lower π-π interactions in compound **3**. Similar absorbance behaviors were observed for compounds **2** and **4** systems.

The fluorescence spectra of **1**-**4** in aqueous solution are shown in Fig. 6. The maximal emission band of compounds 3 and 4 are 552 nm and 547 nm, respectively. The fluorescence quantum yields of compounds **1** and **2** are distinctively reduced about 81% and 98% relative to that of compounds **3** and **4** because of the introduction of H^+. All the changes could be interpreted as stronger π-π interactions in **1** and **2**. As carboxyl substituted derivatives, **3** and **4** were comparative electron donors of **1** and **2**. The additional electron accepter interaction strengthened the π-π interactions, resulting in a dominant π-π stacking in **1** and **2**. Correspondingly, the π-π stacking in **3** and **4** played a less important role in the water. Therefore, both of the emission intensities of **3** and **4** were quenched by π-π stacking produced by H^+ at carboxyl group.

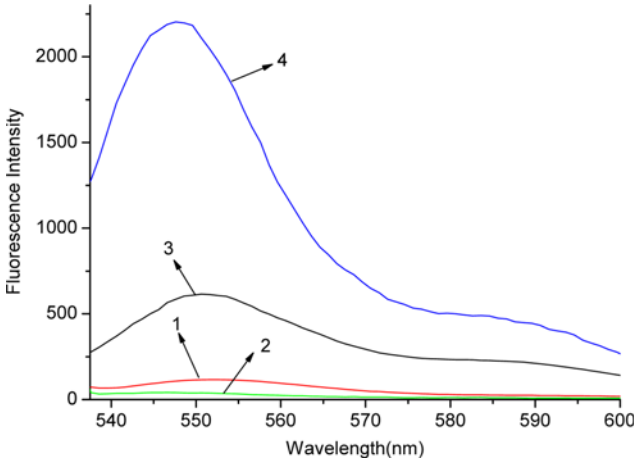

Fig. 6. Comparison of the fluorescence spectrums of compounds 3 and 4 with that of compounds 1 and 2 in aqueous solution (10^{-5} M) (The excitation wavelength was 533 nm for 1, 3 and 544 nm for 2, 4).

3. DFT Calculations

To enhance the understanding of the relationship between the molecular structures and electronic properties of compounds **1** and **2**, structure optimizations and molecular orbital (MO) calculations based on a simplified model were carried out with density functional theory (DFT) at the B3LYP/6-31G* level. The calculated molecular orbital (HOMO and LUMO) energies are shown in Table 1. The minimized structure is shown in Fig. 7 and the calculated frontier molecular orbital maps are shown in Fig. 8. Model compound PTCDA has also been calculated for comparison.

The molecular energy levels of the frontier molecular orbital revealed that the introduction of imide group has raised the energy

Table 1. Calculated and experimental parameters of compounds 1, 2 and PTCDA

Compound	HOMO[a]	LUMO[a]	E_g[a]	λ_{max}	E_g[b]
1	−3.84	−1.39	2.45	533	2.33
2	−3.79	−1.47	2.32	544	2.28
PTCDA	−4.30	−1.36	2.94	-	-

[a]Calculated by DFT/B3LYP (in ev)
[b]At absorption maxima in aqueous solution (Eg=1240/λ_{max})
'-' Stands for no test

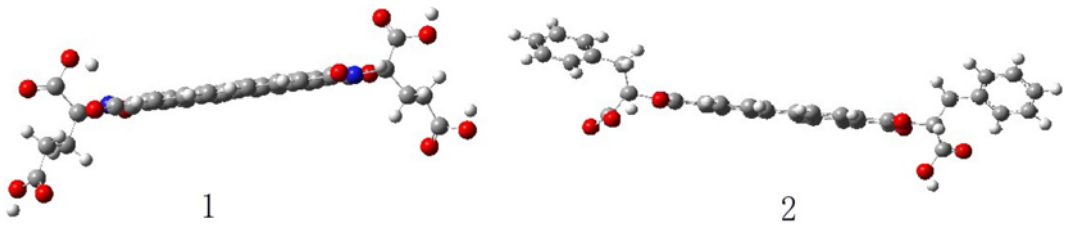

Fig. 7. Optimized structures of compound 1 and 2 obtained by DFT calculations at the B3LYP/6-31G* level.

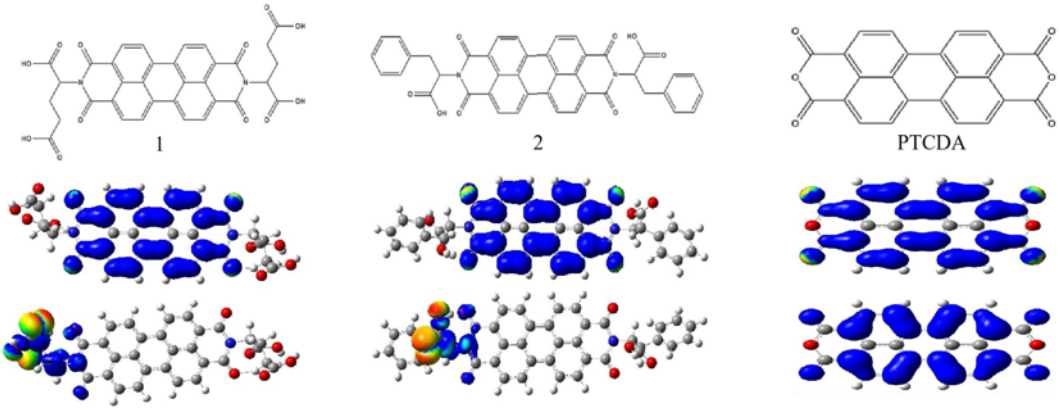

Fig. 8. Computed frontier orbital of compounds 1, 2 and PTCDA (The upper graphs are the LUMO and lower ones are the HOMO).

levels of LUMO for compounds **1** and **2** relative to that of the model compound PTCDA; therefore, the energy gap between HOMO and LUMO decreased significantly. This corresponds well to the experimentally recorded red-shifted absorption spectra of compounds **1** and **2**. It was reported that PASP has absorbance maximum A^{0-0} at 527 nm in pH 7.20 HEPES buffer. According to the TDDFT calculation, the energy gap between HOMO and LUMO was 2.39 ev and the experimental data was 2.35 ev. These data agree well with our experimental result of compound **1** in aqueous solution [19]. As an L-phenylalanine amine substituted derivative, the energy gap of compound **2** between HOMO and LUMO is relative lower than that in compound **1**. Therefore, the absorption maximum in the absorption spectra of compound **2** is in the red side relative to that of compound **1**. Furthermore, the relative band gap energies estimated from the longest absorption maxima of **1**-**2** in aqueous solution are in good agreement with the theoretical calculations. The slight diversion between the calculated values and experimental results from the solvation effects for experiments and gas-phase for theoretical calculations.

The study of the ground-state geometries and electronic structures of PDIs molecules provided preliminary insights into the electronic structures and interactions in these molecular systems. As expected, the minimized structure revealed that the compounds **1** and **2** cores are nearly planar without substituents in the bay positions (Fig. 7). The frontier molecular orbital maps revealed that the HOMO for compounds **1** and **2** were located on the amino acid positions, while the LUMO was entirely delocalized over the perylene rings between the two identical amino acid groups (Fig. 8). The distribution of the HOMO and LUMO suggests that carboxyl group acts as the electron donor and the PDI acts as the electron acceptor. Importantly, the imide group that connected the donors and the acceptors had a small fraction of charge density in both HOMO and LUMO for the dyads, indicating significant interaction between the donor and acceptor moieties. Such orbital partitions are beneficial for electron injection and overall photovoltaic performance.

4. Cell Imaging Experiments

Live cell imaging based on compounds 3 and 4 was investigated with fluorescence microscopy. The fluorescence images of stained cells are shown in Fig. 9. Strong fluorescence from the cellular cytoplasm was observed for hela cells, implying that both compounds 3 and 4 were efficiently internalized by hela cells and accumulated in the cytoplasm. After staining, the living hela cells appeared healthy. Their morphology was devoid of vacuole and any other sign of structural degradation.

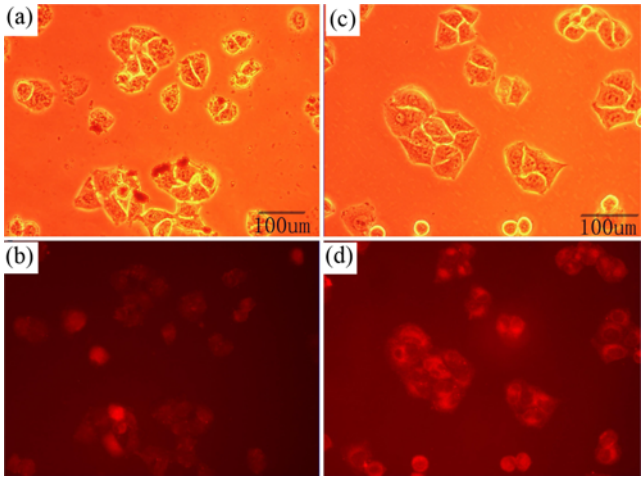

Fig. 9. Fluorescence images of hela cells stained with 10^{-5} M compound 3 ((a), (b)) or 4 ((c), (d)) for 1.0 h ((a), (c): bright field images; (b), (d): fluorescence microscope images).

CONCLUSIONS

We have synthesized two amino acid functionalized water-soluble perylene diimides dyes with long wavelength absorption by introducing L-glutamic amine or L-phenylalanine amine groups at the imide position. Nearly no fluorescence was observed for them in water because of the strong π-π interactions. The compounds can further react with $NH_3 \cdot H_2O$ to form novel dyes which are significantly water-soluble and have very high fluorescent quantum. The molecular energy levels of the frontier molecular orbital revealed that the energy gap between HOMO and LUMO of the new compounds decreased significantly. The distribution of the HOMO and LUMO suggested that carboxyl group acts as the electron donor and the PDI acts as the electron acceptor. Strong fluorescence and

photostability of compounds 2 and 4 in living hela cells were further demonstrated. Good water solubility, high fluorescence quantum yield, low cytotoxicity, and photostability make these perylene diimide dyes excellent candidates for probes in living cell imaging.

ACKNOWLEDGEMENTS

Financial support was received from National Major Projects on Control and Management of Water Body Pollution (Grant No. 2012ZX07404-003-006), and the Natural Science Funds of Shandong Province of China (Grant No. Y2007B42).

REFERENCES

1. M. Wasielewski, *J. Organic Chem.*, **71**, 5051 (2006).
2. H. Langhals, *Chim. Acta,* **88**, 1309 (2005).
3. C. Li and H.Wonneberger, *Adv. Mater.*, **24**, 613 (2012).
4. Y. Ma, F. Zhang, P. Li, J. Wu and H. Ren, *Chin. J. Anal. Chem.*, **40**, 77 (2012).
5. W. Tan, X. Li, J. Zhang and H. Tian, *Dyes Pigm.*, **89**, 260 (2011).
6. F. Würthner, *Chem. Commun.*, 1564 (2004).
7. T. Heek, C. Fasting, C. Rest, X. Zhang, F. Würthner and R. Haag, *Chem. Commun.*, **46**, 1884 (2010).
8. F. Bo, B. Gao, W. Duan, H. Li, H. Liu and Q. Bai, *RSC Adv.*, **3**, 17007 (2013).
9. Y. Funda, D. A. Lale, C. Hande, G. Dicle and A. Engin U., *Organic Lett.*, **14**, 2885 (2005).
10. A. Shaller, W. Wang, H. Gan and A. Li, *Angew. Chem. Int. Ed.*, **47**, 7705 (2008).
11. H. Ji, R. Majithia, X. Yang, X. Xu and K. More, *J. Am. Chem. Soc.*, **130**, 10056 (2008).
12. B. Gao, H. Li, H. Liu, L. Zhang, Q. Bai and X. Ba, *Chem. Commun.*, **47**, 3894 (2011).
13. F. Rui, R. Carlos, C. Maria, M. Manuel and F. Maria, *RSC Adv.*, **3**, 24535 (2013).
14. M. Yin, J. Shen, G. O. Pflugfelder, T. Weil and K. Müllen, *J. Am. Chem.* Soc., **130**, 7806 (2008).
15. A. Becke, *J. Chem. Phys.*, **98**, 5648 (1993).
16. A. Becke, *Phys. Rev. A*, **38**, 3098 (1998).
17. K. Ong, J. Jensen and H. Hameka, *J. Mol. Struct.: THEOCHEM*, **459**, 131 (1999).
18. C. Liu, X. Zhang and M. Wang, *J. of Natural Science of Heilongjiang University*, **24**, 522 (2007).
19. L. Zhong, F. Xing, W. Shi, L. Yan, L. Xie and S. Zhu, *Appl. Mater. Interfaces*, **5**, 3401 (2013).
20. K. Erika, K. Dariusz, C. Marinella, L. Silvia, F. Antonino and B. Fabio, *Dyes Pigm.*, **99**, 329 (2013).
21. C. Huang, S. Barlow and S. Marder, *J. Org. Chem.*, **76**, 2386 (2011).
22. Y. Li, W. Han and M. Liao, *Acta Phys. Chim. Sin.*, **25**, 2493 (2009).
23. L. Liu and X. Zhang, *Acta Phys. Chim. Sin.*, **28**, 283 (2012).